Journal of Hazardous Materials 180 (2010) 552–560

Contents lists available at ScienceDirect

Journal of Hazardous Materials

journal homepage: www.elsevier.com/locate/jhazmat

Adsorption of heavy metals onto activated carbons derived from polyacrylonitrile fiber

Muhammad Abbas Ahmad Zaini[a,c,*], Yoshimasa Amano[a,b], Motoi Machida[a,b]

[a] Graduate School of Engineering, Chiba University, Yayoi-cho 1-33, Inage-ku, Chiba 263-8522, Japan
[b] Safety and Health Organization, Chiba University, Yayoi-cho 1-33, Inage-ku, Chiba 263-8522, Japan
[c] Department of Chemical Engineering, Universiti Teknologi Malaysia, 81310 Skudai, Johor, Malaysia

ARTICLE INFO

Article history:
Received 13 January 2010
Received in revised form 13 April 2010
Accepted 15 April 2010
Available online 22 April 2010

Keywords:
Activated carbon
Adsorption
Desorption
Heavy metals
Polyacrylonitrile fiber

ABSTRACT

The aim of this research is to produce activated carbons derived from polyacrylonitrile (PAN) fiber and to examine their feasibility of removing heavy metals from aqueous solution. Thermogravimetric analysis was used to identify the suitable conditions for preparing oxidized fiber and coke as activated carbon precursors. Steam and CO_2 were used to activate the precursors. Activated carbons were characterized by their pore texture, elemental compositions and surface functionalities. Batch adsorption and desorption studies were carried out to determine the metal-binding ability of activated carbons. Two commercial activated carbon fibers (ACFs), i.e., A-20 and W10-W, were employed to compare the removal performance of PAN derived activated carbons. Influence of oxidation treatment of PAN fiber prior to steam activation was also explored and discussed. Results indicated that steam produced a higher surface area but a lower resultant yield as compared to CO_2. Also, precursors activated by steam showed a greater removal performance. For both activation methods, fiber displayed a better metal-binding ability than coke. A small nitrogen loss from PAN fiber as a result of oxidation treatment assisted a greater removal of Cu(II) and Pb(II), but the interaction to Cu(II) was found stronger. It is proposed that the formation of cyclized structure by oxidation treatment minimized the nitrogen loss during steam activation, hence increased the uptake performance.

1. Introduction

There has been increasing concern over the presence of toxic metal ions in receiving water from metal-finishing or electroplating industry [1]. Heavy metals can easily enter the food chain because of their high solubility in water. These non-biodegradable species have been proven hazardous and tend to cause a number of health problems, diseases and disorders [2]. Industrialists have now been looking for effective measures to comply with stringent contaminant limit set by the World Health Organization (WHO) [1,2].

Adsorption by activated carbon, by far, has become a method of choice to offset this problem. Adsorption becomes a preferred choice than other physico-chemical techniques of heavy metal remediation due to its simplicity, cheap, easy to scale-up and most importantly able to remove low concentration substance even at part per million levels with high efficiency [1,3]. Activated carbon has been widely used in water treatments because of its high specific surface area, chemical stability and durability [3]. Its utilization for heavy metals adsorption greatly relies upon surface acidity [4,5] and special surface functionality [6–8], where the removal mechanisms may comprise of ion-exchange [4,5], basal plane–cation interaction [4] and coordination to functional groups [6,7].

In recent years, considerable interest has been shown to a new category of activated carbon in the form of fiber [9,10]. Activated carbon fiber (ACF) is noted to possess a bigger bulk volume than the ordinary pelletized or powdered activated carbon, thus giving a fast adsorption and desorption rates [9]. ACF can be produced from coal [11] and petroleum pitches [12,13], rayon [14], polyacrylonitrile (PAN) [15–17] and phenolic resin [18] through high temperature gasification in steam or CO_2. Ko et al. [19] reported that steam was better than CO_2 for generating a well-distributed surface area of ACF. Chemical activation by NaOH, KOH, H_3PO_4 or $ZnCl_2$, however, has not been recommended because despite enhancing the porosity, the reagent may also destroy the fiber morphology [17,20].

Nowadays, PAN based ACF (PAN-ACF) has attracted much attention from many researchers due to its high adsorption performance as compared to other counterparts. A number of studies have been focused on the preparation of PAN-ACF from its raw precursor, where the values of specific surface area varying from 500 to 900 m^2/g [15,17,21]. In other development, a great concern has

* Corresponding author. Present address: Universiti Teknologi Malaysia, 81310 Skudai, Johor, Malaysia. Tel.: +6 07 5535552.
E-mail address: abbas@fkkksa.utm.my (M.A.A. Zaini).

0304-3894/$ – see front matter © 2010 Elsevier B.V. All rights reserved.
doi:10.1016/j.jhazmat.2010.04.069

been shown on the removal of organic compounds [9,18,22] and air pollutants [17,23]. However, there is little information concerning the use of PAN-ACF to remediate metal-contaminated wastewater in much of the published literature.

The present work is devoted to prepare activated carbons from PAN fiber and to evaluate their metal-binding ability. Steam and CO_2 were used to activate the precursors. A-20 and W10-W, two commercially available ACFs were employed for comparative studies. Textural characteristics, elemental properties and surface functional groups of each sample were correlated with the adsorption and desorption performances. The influence of oxidation treatment prior to steam activation was also examined and discussed.

2. Materials and methods

All analytical-reagent grade chemicals were purchased from Kanto Chemical Co., Inc. As-received petroleum pitch based activated carbon fibers namely A-20 and W10-W were purchased from Unitika, Ltd. PAN fiber (69.9% C, 4.73% H, 25.4% N; 2.32% moisture) was obtained from Toray Corporation, Japan. Model solutions containing metal ions were prepared by dissolving the desired weight of $CuCl_2{\cdot}2H_2O$ and $PbCl_2$ in de-ionized water.

2.1. Oxidation and activation procedures

Thermogravimetric analysis was performed using a Seiko EXSTAR6000 TG/DTA6200 instrument to determine the oxidative behaviors and to identify the suitable conditions for preparing oxidized fiber and coke from PAN fiber. About 12 mg PAN fiber was used for each analysis. The flow rate of gas was fixed at 300 mL/min and the heating rate was set at 10 °C/min up to 400 °C. Two different mediums (N_2 and air) and two different temperature settings (long and short) were imposed. The long temperature setting took about 20 h, at which the longest retention was at 195 °C for 9 h, followed by 205 and 215 °C for 2 h, respectively. For short temperature setting, the only retention was at 400 °C for 10 min.

In actual oxidation process, PAN fiber was treated in air at various temperatures ranging from 195 to 280 °C for 3–4 days, depending on the amount of fiber employed. This stage is very critical and special attention needs to be given in order to avoid the fiber from shrinking and melting that will change its morphology [21,24]. Once the oxidized fiber is prepared at 280 °C, further treatment at a higher temperature can be done without changing its physical structure. The coke was prepared by heating the PAN fiber at 280–300 °C, and retained until smoke evolved and the fiber completely shrunk to a metal-like coke deposits. The coke was then ground to a powder form prior to activation.

The fiber was detached to obtain even distribution of surface area during activation. About 1.5 g of oxidized fiber was placed at the center of a quartz tube inside a tubular furnace. N_2, a carrier gas, was introduced at a flow rate of 80 mL/min. Water at a flow rate of 13.5 mL/h was injected at the upstream of the quartz tube using an Eyela micro tube pump (Tokyo Rikakikai Co., Ltd.) once the desired temperature was attained. Water was immediately evaporated to steam when reaching the activation chamber and the process was held for the desired activation time. The sample was cooled to room temperature under N_2 flow at the end of activation. The optimum activation conditions were determined by varying temperature from 600 to 850 °C and time from 15 min to 1 h. The resultant steam-activated PAN fibers were dried in an oven at 115 °C for 1 h to remove remaining moisture and then stored in desiccators. The coke of PAN fiber was activated by steam under the optimum activation conditions.

Procedures employed for CO_2 activation has been described by Jia et al. [6]. Briefly, the oxidized fiber and coke were activated at 900 °C for 1 h under a CO_2 flow rate of 300 mL/min.

Activated carbons derived from PAN fiber were designated as PS60-80, CS80, PC90 and CC90. The first alphabet refers to physical appearance (P: PAN fiber, C: coke), and the second alphabet indicates the activation method (S: steam, C: CO_2), while the last two numerals represent the activation temperature (for example 90: 900 °C).

The oxidized fibers were subjected to oxidation treatment in air flow of 300 mL/min using a tubular furnace at temperatures between 300 and 450 °C for 30 min. The treated oxidized fibers are designated as P30-45, where the last two numerals represent the oxidation temperature (for example 30: 300 °C). These treated oxidized fibers were activated by steam at 800 °C for 15 min under the same previously mentioned N_2 and water flow settings. The resultant steam-activated PAN fibers were defined as P30S-P45S, where the last alphabet refers to steam activation.

2.2. Characterization of activated carbons

Textural characteristics of activated carbon were obtained at liquid nitrogen temperature of −196 °C using a Beckman Coulter SA3100 surface area analyzer (USA). The activated carbons were out-gassed in vacuum at 300 °C for 2 h prior to measurement. The surface area of activated carbons was estimated by BET (Brunauer–Emmett–Teller) model with assumption that the adsorbed nitrogen molecule having the cross sectional area of 0.162 nm^2, while the total pore volume was determined at relative pressure, P_s/P_o of 0.9814. Micropore volume and mesopore surface area were obtained from the *t*-plot method. Mesopore volume can be calculated by subtracting micropore volume from total pore volume. Average pore width can be roughly calculated from BET surface area and total pore volume.

Elemental compositions were measured twice using a Perkin-Elmer PE2400 microanalyzer. The samples were dried at 115 °C for 2 h to remove physisorbed moisture prior to measurement.

Surface chemistry was determined using Boehm titration methods [25]. Different batches of 150 mg activated carbons were brought into contact with 15 mL solutions of 0.1 M $NaHCO_3$, 0.05 M Na_2CO_3, 0.1 M NaOH and 0.1 M HCl. The mixtures were retained in a mechanical agitator at 100 rpm and 25 °C for 48 h. Then, the aliquots were back-titrated with either 0.05 M HCl for acidic groups or 0.1 M NaOH for basic groups. Neutralization points were observed using two universal pH indicators, i.e., phenolphthalein for titration of strong base with strong acid, and methyl red for weak base with strong acid. The amount of each functional group was calculated with assumptions that $NaHCO_3$ neutralizes only carboxylic groups, Na_2CO_3 neutralizes carboxylic and lactonic groups, and NaOH neutralizes carboxylic, lactonic and phenolic groups, while HCl neutralizes basic groups [25].

2.3. Batch adsorption and desorption experiments

Thirty milligrams of activated carbon was added to conical flasks containing 50 mL metal ions solutions of a relatively high concentration. The selected concentrations for Cu(II) and Pb(II) were 20 and 40 ppm, respectively [2,6]. The solution pH was left unadjusted, and was measured as 5.2 ± 0.2. Adsorption of metal ions was carried out at 25 °C for 48 h in a stirred batch system.

Few drops of 0.1 M HCl were added to supernatant to stabilize the metal ions. The concentration of metal ions was measured using an atomic absorption spectroscopy (AAS) model Rigaku novAA 300. The amount of metal ions adsorbed by activated carbon in mmol/g was calculated as $(C_o - C_e) \times (V/m)$, where C_o and C_e are respectively the initial and equilibrium concentrations in mmol/L, V in

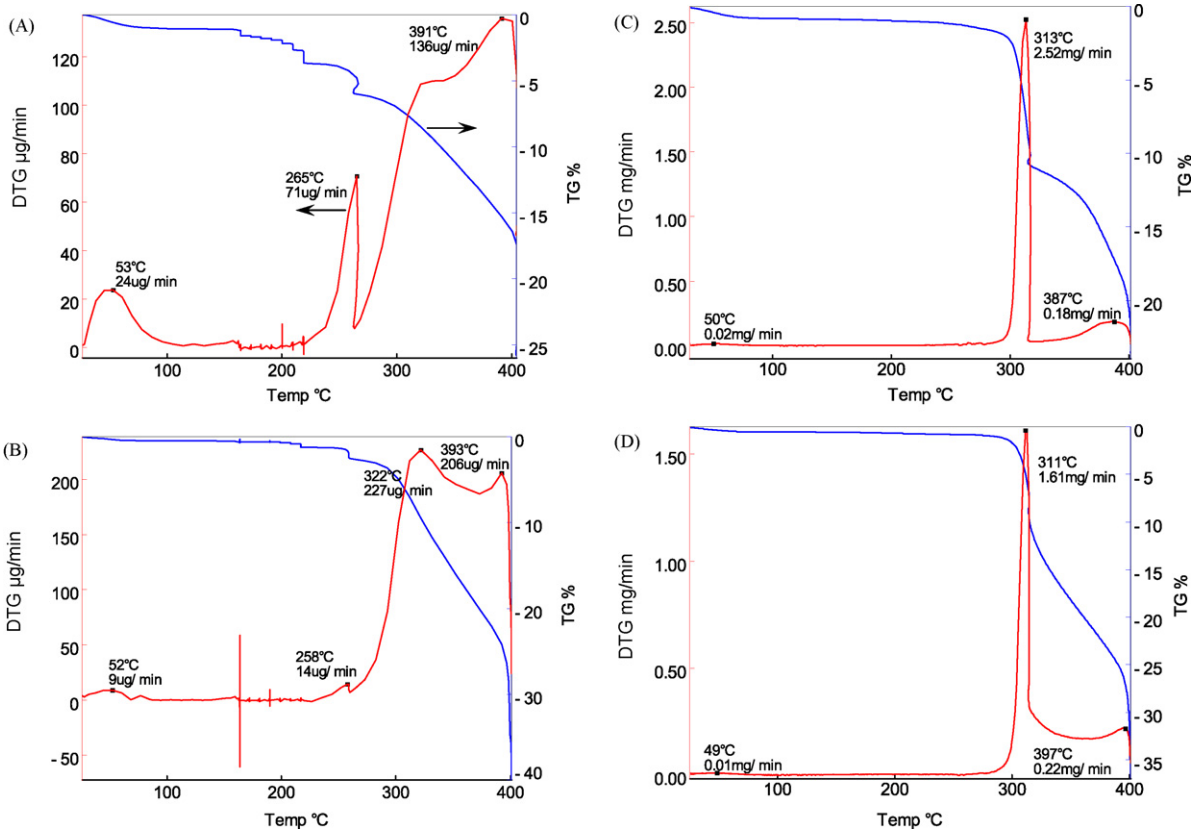

Fig. 1. TG and DTG curves of long (A and B) and short (C and D) temperature settings of PAN fiber in air (A and C) and N_2 (B and D).

L is the volume of solution and *m* in g is the mass of activated carbon.

Solutions already used for adsorption were decanted and conical flasks containing spent activated carbons were thereafter filled with 50 mL fresh de-ionized water for desorption studies. The procedures and settings are the same as described for adsorption. There was also a need to adjust the solution pH of Pb(II) to 3.7 because of precipitation during adsorption. Each experiment was repeated at least 3 times to ensure a good reproducibility of results.

3. Results and discussion

3.1. Oxidation and activation

Thermogravimetric profiles of PAN fiber are shown in Fig. 1. All profiles show a common peak at temperatures between 49 and 53 °C, which corresponds to the release of physisorbed moisture. Clearly the intensity of the aforementioned peak in air flow (A and C) is greater than that of N_2 (B and D) because the fiber tends to adsorb moisture from air at ambient temperature. Another general feature is a peak at temperatures ranging from 387 to 397 °C, which can be attributed to the degradation of material and further strip of volatiles. Under long temperature settings, PAN fiber reveals a high intensity peak at 265 °C in air (A) as compared to that of inert (B). The former could be assigned to the removal of CO_2 and HCN, while only small amount of HCN and NH_3 is released for the latter [26,27]. The presence of a high intensity peak in N_2-treated PAN fiber (B) at 322 °C, however, indicates an autocatalytic exothermic reaction that results in the shrinking and melting of the fiber to form coke deposits. This phenomenon also exists under short temperature settings (C and D) over the temperature range of 311–313 °C, where the sharp peaks of high intensity can be observed. More volatile products are liberated once the coke is formed thus causing a greater weight loss. Inappropriate oxidation treatment in nitrogen (B and D) may result in a greater weight loss particularly when the coke is produced [27].

PAN fiber treated under long temperature setting in air was found suitable to prevent the formation of metal-like coke deposits so as to withstand high temperature activation. However, in actual oxidation condition, the amount of fiber used was much greater than that of thermogravimetric analysis. Thus, the settings for time and temperature were adapted to the quantity used. Approximately 3–4 days were required to produce oxidized PAN fiber from 195 °C to a final temperature of 280 °C. Frequent monitoring and mixing were necessary because the fiber usually not uniformly oxidized and easily shrunk.

Effect of temperature in steam activation of oxidized fiber on BET surface area and yield is given in Fig. 2. Three to four indepen-

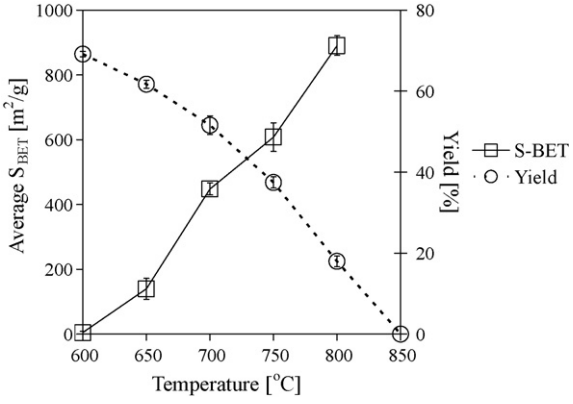

Fig. 2. Effect of temperature on BET surface area and yield in steam activation of PAN fibers (water flow: 13.5 mL/h, nitrogen flow: 80 mL/min, duration: 30 min).

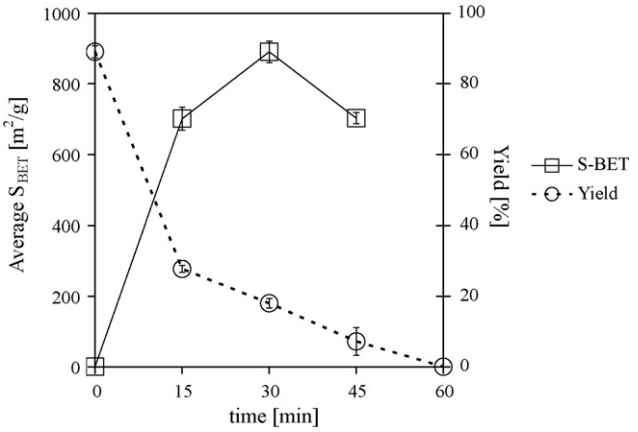

Fig. 3. Effect of time on BET surface area and yield in steam activation of PAN fibers (water flow: 13.5 mL/h, nitrogen flow: 80 mL/min, T: 800 °C).

dent BET measurements with at least two reproductions produce a 7–10% deviation from the average values. The BET surface area was found to increase with increasing temperature. At 850 °C, the oxidized fiber was completely vanished to volatiles, while at 600 °C, although the burn-off was only 30%, there was only a small pore development generated by steam. The highest recordable value of surface area was obtained at 800 °C. At a higher temperature, the linear structures of PAN are expected to coalesce to form a denser graphite basal plane. It is clear that water molecules of steam not only serve as activating agent to increase the surface area, but also degrade the fiber at a higher temperature.

Effect of time in steam activation is shown in Fig. 3. The BET surface area reached its optimum after 30 min activation, with a value of 886 m^2/g and 18% yield. In addition, the yield was decreased with increasing activation time where the fiber was completely destroyed after 60 min. The decrease of surface area after 45 min activation was an early sign of fiber decomposition by steam at 800 °C.

3.2. Characteristics of activated carbon

Characterization of activated carbon is important to understand the properties that may affect the removal of metal ions. Fig. 4 shows the N_2 adsorption–desorption isotherms of activated carbons derived from PAN fiber, and two commercial ACFs (A-20 and W10-W). All activated carbons exhibit a convex upward isotherm with steep slope at low P_s/P_o, which is indicative of a highly microporous material. According to IUPAC classification [28], these activated carbons can be described under type I isotherm with a small type H4 hysteresis, which is associated with a narrow pore size distribution of microporous material with plate-like pores. Visibly, A-20 and W10-W possess a higher surface area than activated carbons derived from PAN fiber because of a greater volume adsorbed as P_s/P_o approaching unity.

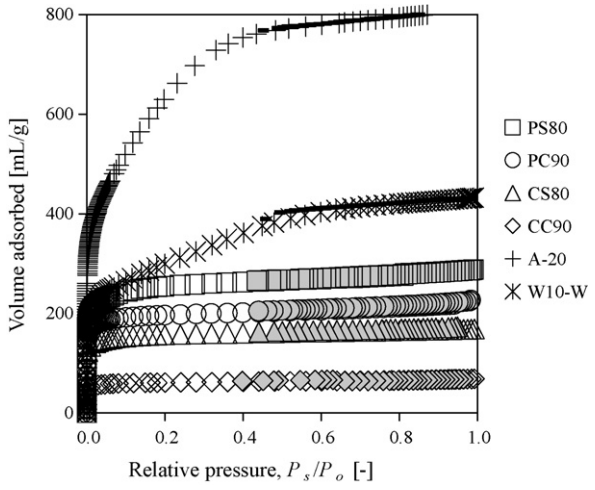

Fig. 4. N_2 adsorption–desorption isotherms of activated carbons derived from PAN fiber and commercial ACFs. Closed symbols and solid lines represent the desorption branch.

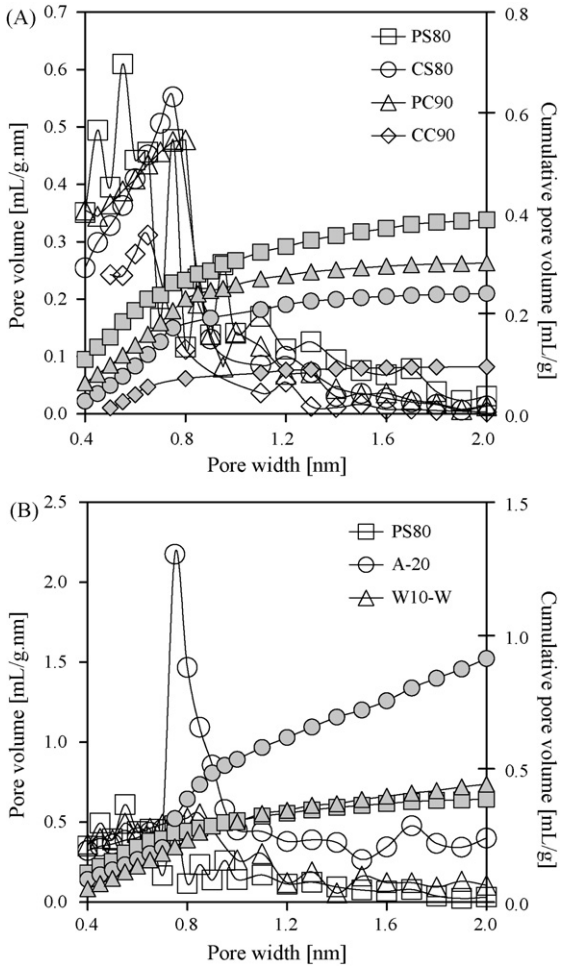

Fig. 5. Pore size distributions of (A) activated carbons derived from PAN fiber and (B) commercial ACFs. Open symbols represent differential pore volume, closed symbols represent cumulative pore volume.

Textural characteristics and yield of activated carbons are listed in Table 1. It is evident that steam was effective to produce a greater surface area and pore volume, but the resultant yield was lower than that of CO_2 for both oxidized fiber and coke. A higher degradation of material by steam is due to a rapid burn-off by water molecules although the activation temperature was 100 °C lower than that of CO_2.

Coke showed a somewhat lower surface area than fiber even under the same activation procedures because of the effect of autocatalytic reaction that affects the development of porosity. A-20 and W10-W possess a significantly high surface area of 2312 and 1060 m^2/g, respectively. The average pore widths of all samples are within the upper limit of micropores to the lower limit of mesopores varying from 1.9 to 2.5 nm [29].

In depth analysis of pore size distribution is given in Fig. 5. The curves were constructed based on the report by Horvath and Kawazoe [30], which is also known as H-K method. Different from

Table 1
Textural characteristics of activated carbons derived from PAN fiber and commercial ACFs.

Carbon	Yield (%)	Pore characteristics					
		S_{BET} (m^2/g)	S_{mi} (m^2/g)	V_{total} (mL/g)	V_{mi} (mL/g)	R_{me} (%)	D_{avg} (nm)
PS80	18.0	886	781	0.444	0.349	21.3	2.00
PC90	36.6	675	612	0.348	0.278	20.2	2.06
CS80	34.0	536	490	0.260	0.224	14.1	1.94
CC90	42.4	207	194	0.106	0.087	17.4	2.04
A-20	–	2312	2115	1.25	1.06	15.2	2.17
W10-W	–	1060	933	0.667	0.539	19.2	2.52

S_{BET}: BET surface area; S_{mi}: micropore surface area; V_{total}: total pore volume; V_{mi}: micropore volume; R_{me}: mesopore content; and D_{avg} ($4V_{total}/S_{BET}$): average pore width.

Table 2
Results of elemental analysis and surface chemistry of activated carbons.

Carbon	Elemental composition (wt%)				Surface functional groups (mmol/g)					
	Carbon	Hydrogen	Nitrogen	Oxygen[a]	Carboxylic	Lactonic	Phenolic	Total acidic	Basic	Sum
PS80	74.2	1.29	4.20	20.3	0	0	0.225	0.225	1.16	1.39
PC90	79.3	0.99	11.9	7.81	0	0	0.475	0.475	1.21	1.69
CS80	81.1	0.62	11.1	7.18	0	0	0.185	0.185	1.04	1.23
CC90	82.0	0.70	11.7	5.60	0	0	0.190	0.190	0.624	0.814
A-20	94.6	0.02	0.44	4.94	0	0	0.375	0.375	0.321	0.696
W10-W	90.1	0.04	0.50	9.36	0.09	0.08	0.315	0.485	0.019	0.504

[a] Calculated by difference.

other derived activated carbons, PS80 shows a multimodal distribution, concentrated at the supermicropore (0.45 and 0.55 nm) and micropore (0.75–0.95 nm) regions. A similar bimodal distribution is revealed by PC90, CC90 and CS80, where the pores centered at the supermicropore region. A sharp distribution at 0.75 nm is displayed by A-20, while W10-W exhibits a broad multimodal distribution with the highest peak at 0.85 nm. The values of micropore volume predicted from the *y*-intercept of cumulative pore volume in Fig. 5 are almost identical with those estimated by *t*-plot method in Table 1.

Results of Boehm titration and elemental analysis are tabulated in Table 2. It is obvious that A-20 and W10-W contain a higher composition of carbon but a lower proportion of nitrogen as compared to activated carbons derived from PAN fiber. A relatively high proportion of hydrogen in PS80 could be attributed to a partially completed graphitic structure. About 58–84% nitrogen loss was observed from the resultant activated carbons, and this was found significant in PS80 probably due to two possibilities. Firstly, steam effectively removes nitrogen molecules from the carbon surface even the activation temperature was lower than that of CO_2, and secondly, the oxidized fiber produced at 280 °C may contain a plenty of non-cyclized nitrogen that is prone to liberate at a lower temperature. On the contrary, the formation of coke as a result of exothermic reaction may assist the cyclization that may prevent the release of nitrogen functionalities in activation [24]. The increase of oxygen content in PS80 was due to the reaction of water molecules in steam with carbon atom at the edges of basal plane [15]. Oxygen complexes are predicted to be basic in nature and may comprise of carbonyl groups including ketones and pyrones [31,32].

From Table 2, it is evident that PAN derived activated carbons were mainly basic due to the absence of principal surface acidic functional groups, namely carboxylic and lactonic groups. The presence of phenolic groups, however, signifies the interaction between the reactive carbon surface and moisture in air after activation. The basicity of activated carbon, in general, is attributed to delocalized π-electrons and electron-donating groups that can behave as Lewis bases. A considerable amount of carboxylic and lactonic groups in W10-W, enable it to be distinguished from PAN derived activated carbons in adsorption and desorption studies.

Tables 3 and 4 compile the properties of steam-activated PAN fibers that formerly underwent the oxidation treatment at different temperatures. It is worth pointing out that steam activation for the treated fibers was progressed at 800 °C for 15 min. Thirty minutes of activation seems inappropriate because the treated oxidized fibers were easily degraded at a higher temperature. This can be seen in Table 3, where the oxidation treatment results in the increasing burn-off and mesopore content especially when the temperature rises to 400 and 450 °C. The variation of surface area amongst the steam-activated PAN fibers was 10–15%, which is in agreement with that shown in Fig. 3. With a slight deviation in surface area, the influence of oxidation treatment on the removal of metal ions can be easily carried out.

From Table 4, the decrease of H/C ratio of raw PAN fiber in oxidation treatment could be attributed to the dehydrogenation of PAN linear structures to form heterocyclic aromatic structures.

Table 3
Yield and textural characteristics of steam-activated PAN fibers formerly treated at different oxidation temperatures.

Carbon	Yield P (%)	Yield A (%)	W_a/W_p	Pore characteristics					
				S_{BET} (m^2/g)	S_{mi} (m^2/g)	V_{total} (mL/g)	V_{mi} (mL/g)	R_{me} (%)	D_{avg} (nm)
P30S	83.3	29.8	0.358	676	606	0.345	0.276	20.1	2.04
P35S	79.5	26.9	0.338	681	614	0.351	0.277	21.0	2.06
P40S	60.0	13.8	0.230	795	700	0.407	0.314	22.9	2.05
P45S	53.5	9.37	0.175	711	604	0.394	0.270	31.5	2.24

Yield P: post-oxidation yield; Yield A: activation yield; and W_a/W_p: product ratio of activation and post-oxidation.

Table 4
Elemental compositions of PAN fiber, treated oxidized fibers and steam-activated PAN fibers.

Sample	Elemental composition (wt%)				Atomic ratio		
	Carbon	Hydrogen	Nitrogen	Oxygen[a]	H/C	N/C	O/C
PAN	69.9	4.73	25.4	0	0.068	0.364	0
P30	57.6	2.43	20.0	20.0	0.042	0.346	0.347
P35	57.2	1.86	20.8	20.1	0.032	0.364	0.351
P40	55.6	1.61	22.8	20.0	0.029	0.410	0.359
P45	53.9	1.43	26.6	18.2	0.027	0.493	0.337
P30S	70.6	1.36	7.46	20.6	0.019	0.106	0.292
P35S	73.2	0.91	8.22	17.7	0.012	0.112	0.242
P40S	69.1	1.49	6.78	22.6	0.022	0.098	0.327
P45S	67.2	1.31	15.2	16.4	0.020	0.226	0.243

[a] Calculated by difference, H/C: hydrogen to carbon; N/C: nitrogen to carbon; and O/C: oxygen to carbon.

Dehydrogenation is expected to continue in steam activation due to the graphitization process. Oxygen complexes were integrated with PAN fiber to form a stable structure during oxidation treatment, thus increased the O/C ratio. However, a part of these oxygen functionalities probably diminished in steam activation [15] or may evolve again once the reactive surface is exposed to air.

Obviously, P45S gives the highest value of nitrogen content. It is suggested that the degree of cyclization and conjugation can prevent the further elimination of nitrogen during activation. Similarly, the remaining nitrile or amine functional groups in the non-cyclized structures can be easily released at 800 °C, thus decreasing the N/C ratio. Notwithstanding that the elimination of some nitrogen moieties during graphitization process is inevitable because of the crosslinking and polycondensation reactions among the stable structures of PAN. Song et al. [22] described the nitrogen functionalities of PAN based activated carbon fiber as pyridinic, pyrrolic, quaternary nitrogen and nitrogen oxide.

The above explanations can be visualized in Fig. 6. To give a clear picture, this schematic only focused on the possible changes of nitrile of PAN linear structure, where the other potential functionalities including carbonyl and phenolic groups were purposely excluded. It is estimated that the loopholes of missing delocalized π-electrons were produced in the activation of oxidized fibers initially treated at 300–350 °C. This definitely results in the imperfect formation of graphitic structure. Conversely, a near-ideal graphitization can be anticipated in the activation of polymer ladder structures of oxidized fibers previously treated at 400–450 °C.

3.3. Adsorption and desorption studies

Fig. 7 shows the adsorption and desorption profiles of (A) 20 ppm Cu(II) and (B) 40 ppm Pb(II) by steam-activated PAN fibers (PS-series). The growing trend of adsorption and desorption is related to the increase of surface area as the activation temperature increases. PS80 shows the highest uptake capacity of Cu(II) and Pb(II) of 0.19 and 0.22 mmol/g, respectively. PS60, having the surface area of 4.86 m^2/g (Fig. 2), exhibits the lowest removal capacity of Cu(II) and Pb(II) of 0.0132 and 0.0080 mmol/g, respectively. PS60 displayed a higher recovery of 88% for Cu(II) and 90% for Pb(II) in comparison with other PS-series activated carbon fibers. About not more than 30% of these metal ions was able to be recovered in desorption by PS80, which infers a strong interaction between the adsorbates and the surface of activated carbon as the surface area increases. In Cu(II) and Pb(II) adsorption, the amount of protons adsorbed increased with increasing surface area, thus increased the solution pH from its initial value. A greater values of desorption pH than that of adsorption in Fig. 7B implies a relatively weaker affinity of PS-series activated carbon fibers towards Pb(II), as protons still adsorbed on their surface in desorption. Moreover, Pb(II) solution bearing PS80 became cloudy in adsorption because of excessive removal of protons. The increase of alkalinity in solution gives a suitable environment for the formation of precipitate complex of $Pb(OH)_2$ at pH 6.6 [33].

Fig. 8 illustrates the adsorption and desorption performances by different activated carbons derived from PAN fiber under the

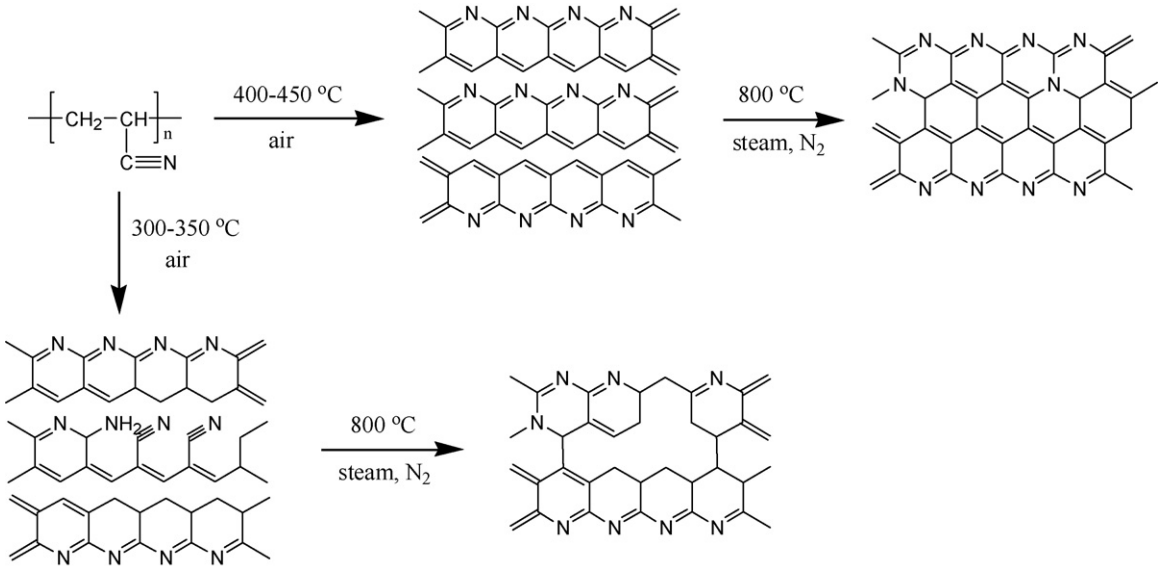

Fig. 6. Possible structural changes of PAN fiber in oxidation treatment and steam activation.

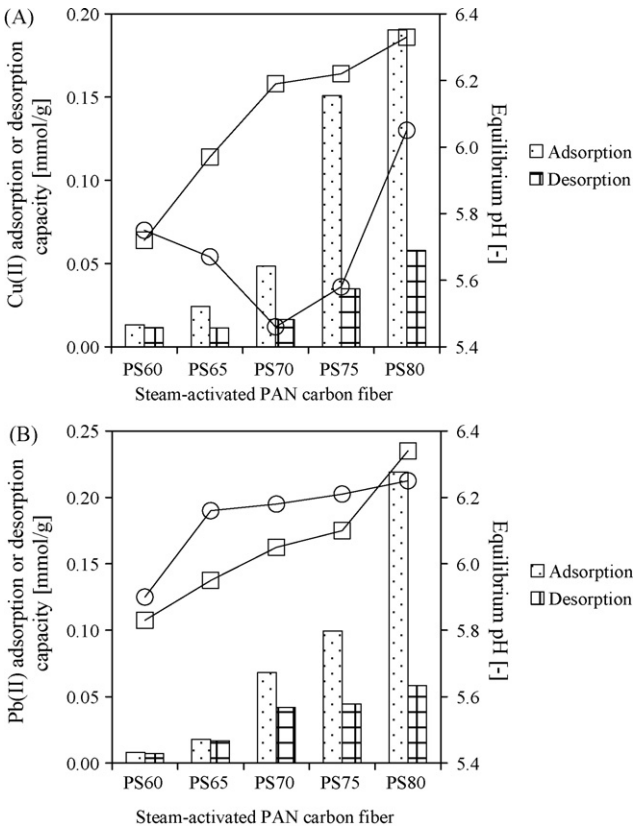

Fig. 7. Adsorption and desorption of (A) 20 ppm Cu(II) and (B) 40 ppm Pb(II) by steam-activated PAN fibers of different activation temperatures. Symbols of adsorption (□) and desorption (○) represent the equilibrium pH at which the final concentration was measured.

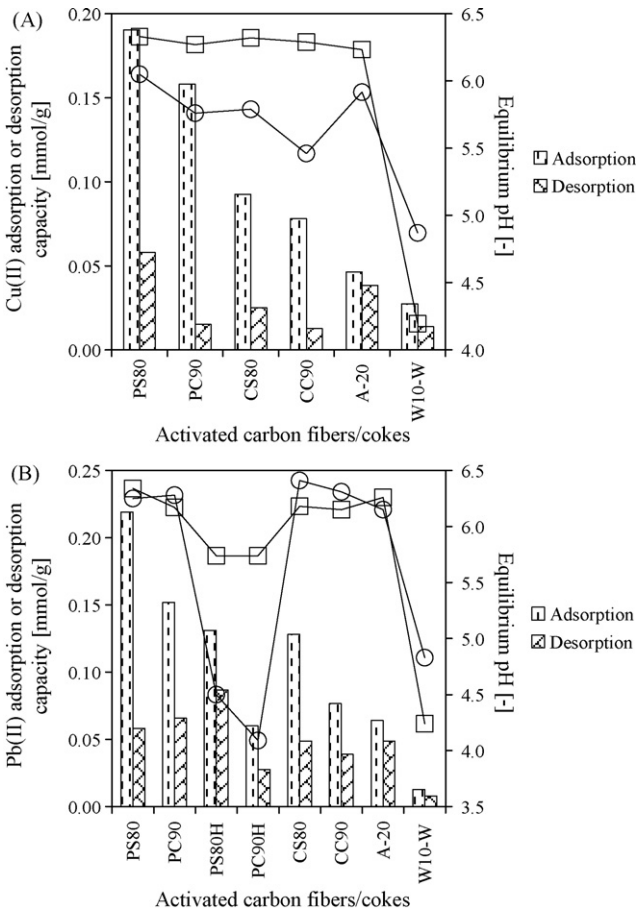

Fig. 8. Adsorption and desorption of (A) 20 ppm Cu(II) and (B) 40 ppm Pb(II) by activated carbons derived from PAN fiber and commercial ACFs. Symbols of adsorption (□) and desorption (○) represent the equilibrium pH at which the final concentration was measured.

same initial concentrations of metal ions. Two commercial ACFs, namely A-20 and W10-W were employed for comparison. In general, PAN-ACFs (PS80 and PC90) show a superior performance than other activated carbons for Cu(II) and Pb(II) removal.

A lower removal capacity by CS80 and CC90 was associated with a smaller BET surface area than PAN-ACFs. Clearly, PS80 showed a greater capacity than PC90, while CS80 gave a better removal than CC90. For both precursors (fiber and coke), steam was found better than CO_2 for generating a higher surface area to accommodate Cu(II) and Pb(II) ions. A-20 and W-10W, however, showed a poor performance in comparison with activated carbons derived from PAN fiber. Although possessing a 2.6 times bigger surface area than PS80, the performance of A-20 was undoubtedly inferior. A-20 displays only 0.0463 and 0.0641 mmol/g for Cu(II) and Pb(II) uptake, respectively, which are 3–4 times lower than that of PS80. Relatively abundant acidic functionalities in W10-W also provide a little contribution on the removal of metal ions as opposed to activated carbons derived from PAN fiber. W10-W shows a lower removal capacity of Cu(II) and Pb(II) as compared to A-20 because of a lower surface area but exhibits a slightly strong interaction to Cu(II) and Pb(II) due to its rich surface acidic functional groups. Yet, a smaller ratio of adsorption to desorption by commercial ACFs in comparison with that of activated carbons derived from PAN fiber signifies a weaker interaction between the adsorbates and the active sites in the absence of nitrogen-rich surface. Therefore, surface area and/or surface acidic functionalities are not the sole factors that may influence the removal of metal ions and its affinity onto the carbon surface. Obviously, the nitrogen-rich content of activated carbons derived from PAN fiber plays a significant role in enhancing the uptake of Cu(II) and Pb(II) ions. It is expected that the removal of these metal ions onto the nitrogen-rich surface was through a coordination mechanism [6,7,34].

In Fig. 8A, PC90 reveals a 3 times bigger ratio of adsorption to desorption than PS80. This is thought to be caused by a higher composition of nitrogen left upon activation in PC90 (Table 2), which provides a strong coordination to Cu(II) ions. From Fig. 8B, Pb(II) precipitation was also occurred by PC90 but the cloudiness of the solution was less intense than that of PS80. In a non-adjusted solution pH, the removal of Pb(II) by PAN-ACFs could be described as a hybrid of adsorption and precipitation. It is noteworthy that the presence of stable precipitate complex decreases the concentration of metal aqua ions, thus partly nullify the amounts of adsorption and desorption. To validate this phenomenon, an acidic solution of pH 3.7 was used in the adsorption and desorption of PAN-ACFs (the results are differentiated by the last alphabet H; PS80H and PC90H). In this case, the solutions remained clear from sediments during adsorption and desorption. Clearly PS80H showed a greater capacity than PC90H, where the equilibrium pH was identical at 5.7. Similar to that of Cu(II) removal, the ratio of adsorption to desorption by PC90H was slightly higher than that of PS80H, even though the solution for desorption was acidic.

Effect of oxidation treatment prior to steam activation on the removal of Cu(II) and Pb(II) is demonstrated in Fig. 9. The removal capacity was found to increase with increasing oxidation temperature, which reflects the rising degree of cyclization and conjugation to form polymer ladder structures. This is associated with the increase of N/C ratio throughout the oxidation treatment. It is evi-

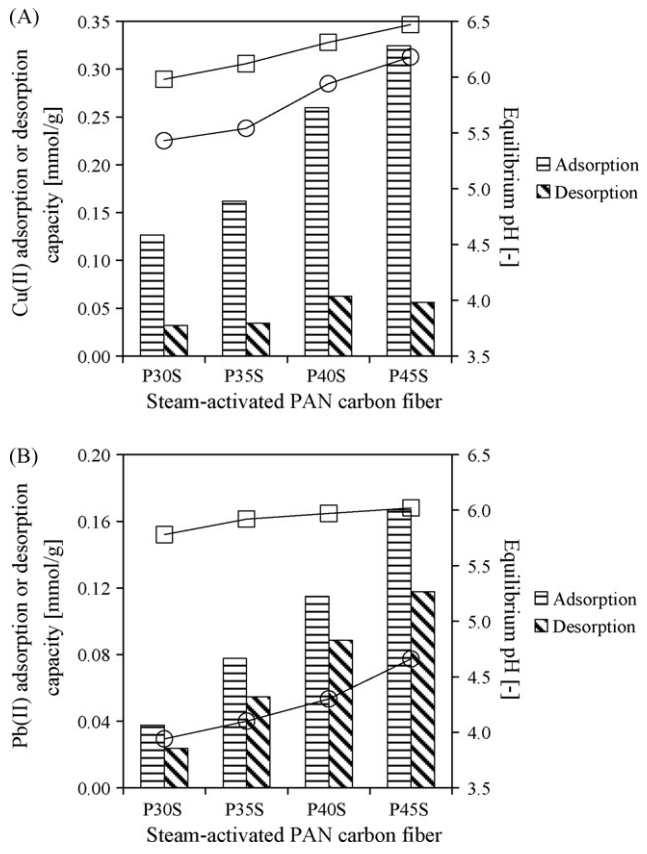

Fig. 9. Adsorption and desorption of (A) 20 ppm Cu(II) and (B) 40 ppm Pb(II) (solution pH 3.7) by steam-activated PAN fibers formerly treated at different oxidation temperatures. Symbols of adsorption (□)) and desorption (○) represent the equilibrium pH at which the final concentration was measured.

dent that the nitrogen content gives a more influence on the uptake of Cu(II) and Pb(II) over the role of surface area. For instance, in Fig. 9A, P45S (S_{BET}: 711 m^2/g; N/C: 0.226) exhibits the highest removal capacity of Cu(II) of 0.32 mmol/g, which is about 68% greater than that of PS80 (S_{BET}: 886 m^2/g; N/C: 0.057). This is also true for Pb(II) adsorption where P45S displayed a removal of about 27% higher than PS80H (Fig. 9B).

From Fig. 9A, it is noted that the higher the N/C ratio, the greater the ratio of adsorption to desorption. P45S showed a higher value of adsorption to desorption of 5.8, 1.5 times higher than that of P30S. This infers that nitrogen moieties not only serve as the active sites but also offer a strong interaction with the adsorbed species, particularly to Cu(II) ions [7,35]. Despite increasing the metal uptake, the increase of N/C ratio also increased the capture of protons. This effect becomes prevalent where Pb(II) solution bearing P45S was precipitated in adsorption although the initial solution pH was already altered to 3.7.

Apart from nitrogen content, phenolic groups and delocalized π-electrons may also involve in the removal of metal species [4]. It can be estimated that the decrease of electron density due to loopholes on the graphitic structure (as visualized in Fig. 6) decreases the Cπ-cation interactions. On the other hand, the presence of considerable amount of nitrogen by a proper oxidation treatment may increase the density of π-system through its electron-donating characteristic, thus increases the removal of metal ions through Cπ-cation interaction. It is clear that, without sufficient nitrogen content, A-20 revealed a trivial adsorption of metal species although exhibits a considerable amount of phenolic group, basic in nature and possesses the highest surface area among the activated carbons studied.

4. Conclusions

The present work demonstrated the feasibility of activated carbons derived from PAN fiber to remove heavy metals from aqueous solution. Two precursors, i.e., fiber and coke, were prepared by oxidation in air under long and short temperature settings, respectively. Activated carbons were derived from these precursors through gasification in steam and CO_2. Activated carbons derived from PAN fiber are highly microporous with pores centered at the supermicropore region. Steam was found better than CO_2 to generate a higher surface area, but results in a lower yield. PAN-ACFs showed a better performance of Cu(II) and Pb(II) removal in comparison with commercial ACFs. High amount of nitrogen content plays a significant role over the effect of surface area and surface acidic functional groups in enhancing the adsorption of Cu(II) and Pb(II) ions. Oxidation treatment prior to steam activation was beneficial to minimize the nitrogen loss. Because the lesser the nitrogen loss upon activation, the greater the removal of metal ions, and the stronger the interaction to the active surface. Cu(II) ions showed a relatively stronger coordination onto the nitrogen-rich surface. PAN-ACF is foreseen to be the candidate of adsorbent in heavy metals remediation from aqueous solution.

Acknowledgements

This study was part of M.A.A. Zaini's doctoral dissertation at Chiba University, Japan. It was funded in part by the Japan Society for the Promotion of Science (JSPS) under Grants-in-aid for Scientific Research (C) (No. 20510072). The author, M.A.A. Zaini, is indebted to Ministry of Higher Education Malaysia and Universiti Teknologi Malaysia for the financial support under *SLAI* program. We also thank Dr. Nagao Keiichi (Head) and Dr. Satoru Nakada of Safety and Health Organization, Chiba University for the encouragement and support on this work.

References

[1] T.A. Kurniawan, G.Y.S. Chan, W.-H. Lo, S. Babel, Physico-chemical treatment techniques for wastewater laden with heavy metals, Chem. Eng. J. 118 (2006) 83–98.
[2] WHO, Guidelines for Drinking Water Quality, World Health Organization, Geneva, 2006.
[3] R.C. Bansal, M. Goyal, Activated Carbon Adsorption, Taylor & Francis, New York, 2005.
[4] S. Sato, K. Yoshihara, K. Moriyama, M. Machida, H. Tatsumoto, Influence of activated carbon surface acidity on adsorption of heavy metal ions and aromatics from aqueous solution, Appl. Surf. Sci. 253 (2007) 8554–8559.
[5] V. Strelko, D.J. Malik, Characterization and metal sorptive properties of oxidized active carbon, J. Colloid Interface Sci. 250 (2002) 213–220.
[6] Y.F. Jia, B. Xiao, K.M. Thomas, Adsorption of metal ions on nitrogen surface functional groups in activated carbons, Langmuir 18 (2002) 470–478.
[7] W. Yantasee, Y. Lin, G.E. Fryxell, K.L. Alford, B.J. Busche, C.D. Johnson, Selective removal of copper(II) from aqueous solutions using fine-grained activated carbon functionalized with amine, Ind. Eng. Chem. Res. 43 (2004) 2759–2764.
[8] M. Pesavento, A. Profumo, G. Alberti, F. Conti, Adsorption of lead(II) and copper(II) on activated carbon by complexation with surface functional groups, Anal. Chim. Acta 480 (2003) 171–180.
[9] M. Suzuki, Activated carbon fiber: fundamentals and applications, Carbon 32 (1994) 577–586.
[10] C. Brasquet, P. Le Cloirec, Adsorption onto activated carbon fibers: application to water and air treatments, Carbon 35 (1997) 1307–1313.
[11] J.A. Maciá-Agulló, B.C. Moore, D. Cazorla-Amoroïs, A. Linares-Solano, Activation of coal tar pitch carbon fibres: physical activation vs. chemical activation, Carbon 42 (2004) 1361–1364.
[12] M.W. Thwaites, M.L. Stewart, B.E. McNeese, M.B. Sumner, Synthesis and characterization of activated pitch-based carbon fibers, Fuel Process. Technol. 34 (1993) 137–145.
[13] E. Vilaplana-Ortego, J.A. Maciá-Agulló, J. Alcañiz-Monge, D. Cazorla-Amorós, A. Linares-Solano, Comparative study of the micropore development on physical activation of carbon fibers from coal tar and petroleum pitches, Microporous Mesoporous Mater. 112 (2008) 125–132.
[14] Y.-C. Chiang, C.-C. Lee, H.-C. Lee, Characterization of microstructure and surface properties of heat-treated PAN-and rayon-based activated carbon fibers, J. Porous Mater. 14 (2007) 227–237.

[15] P.H. Wang, Z.R. Yue, J. Liu, Conversion of polyacrylonitrile fibers to activated carbon fibers: effect of activation, J. Appl. Polym. Sci. 60 (1996) 923–929.
[16] Z. Ryu, J. Zheng, M. Wang, B. Zhang, Nitrogen adsorption studies of PAN-based activated carbon fibers prepared by different activation methods, J. Colloid Interface Sci. 230 (2000) 312–319.
[17] I. Martín-Gullón, R. Andrews, M. Jagtoyen, F. Derbyshire, PAN-based activated carbon fiber composites for sulfur dioxide conversion: influence of fiber activation method, Fuel 80 (2001) 969–977.
[18] K.L. Foster, R.G. Fuerman, J. Economy, S.M. Larson, M.J. Rood, Adsorption characteristics of trace volatile organic compounds in gas streams onto activated carbon fibers, Chem. Mater. 4 (1992) 1068–1073.
[19] T.-H. Ko, W.-S. Kuo, C.-H. Hu, Raman spectroscopic study of effect of steam and carbon dioxide activation on microstructure of polyacrylonitrile-based activated carbon fabrics, J. Appl. Polym. Sci. 81 (2001) 1090–1099.
[20] A.-H. Lu, J.-T. Zheng, Study of microstructure of high-surface-area polyacrylonitrile activated carbon fibers, J. Colloid Interface Sci. 236 (2001) 369–374.
[21] A. Gupta, I.R. Harrison, New aspects in the oxidative stabilization of pan-based carbon fibers: II, Carbon 35 (1997) 809–818.
[22] Y. Song, W. Qiao, S.-H. Yoon, I. Mochida, Q. Guo, L. Liu, Removal of formaldehyde at low concentration using various activated carbon fibers, J. Appl. Polym. Sci. 106 (2007) 2151–2157.
[23] I. Mochida, Y. Korai, M. Shirahama, S. Kawano, T. Hada, Y. Seo, M. Yoshikawa, A. Yasutake, Removal of SOx and NOx over activated carbon fibers, Carbon 38 (2000) 227–239.
[24] M. Surianarayanan, R. Vijayaraghavan, K.V. Raghavan, Spectroscopic investigations of polyacrylonitrile thermal degradation, J. Polym. Sci., Part A: Polym. Chem. 36 (1998) 2503–2512.
[25] H.P. Boehm, Some aspects of the surface chemistry of carbon blacks and other carbons, Carbon 32 (1994) 759–769.
[26] T. Murata, S. Takahashi, Evolved gas analysis of polyacrylonitrile resin and Nylon 6 by a DTA–GC–MS combined system, Mass Spectrosc. 22 (1974) 87–94.
[27] M. Surianarayanan, T. Uchida, M. Wakakura, Evolved gases by simultaneous TG-MS technique and associated thermal hazard in drying of polyacrylonitrile, J. Loss Prev. Process Ind. 11 (1998) 99–108.
[28] K.S.W. Sing, D.H. Everett, R.A.W. Haul, L. Moscou, R.A. Pierotti, J. Rouquerol, T. Siemieniewska, Reporting physisorption data for gas/solid systems with special reference to the determination of surface area and porosity, Pure Appl. Chem. 57 (1985) 603–619.
[29] J. Rouquerol, D. Avnir, C.W. Fairbridge, D.H. Everett, J.H. Haynes, N. Pernicone, J.D.F. Ramsay, K.S.W. Sing, K.K. Unger, Recommendations for the characterization of porous solids, Pure Appl. Chem. 66 (1994) 1739–1758.
[30] G. Horvath, K. Kawazoe, Method for the calculation of effective pore size distribution in molecular sieve carbon, J. Chem. Eng. Jpn. 16 (1983) 470–475.
[31] E. Fuente, J.A. Menéndez, D. Suárez, M.A. Montes-Morán, Basic surface oxides on carbon materials: a global view, Langmuir 19 (2003) 3505–3511.
[32] M. Desaeger, M.J. Reis, A.M. Botelho Do Rego, J.D. Lopes Da Silva, I. Verpoest, Surface characterization of poly(acrylonitrile) based intermediate modulus carbon fibres, J. Mater. Sci. 31 (1996) 6305–6315.
[33] D.R. Lide, CRC Handbook of Chemistry and Physics, 82nd ed., CRC Press, Boca Raton, 2001.
[34] M.A.A. Zaini, K. Yoshihara, R. Okayama, M. Machida, H. Tatsumoto, Effect of out-gassing of ZnCl2-activated cattle manure compost (CMC) on adsorptive removal of Cu(II) and Pb(II) ions, TANSO 234 (2008) 220–226.
[35] M.A.A. Zaini, R. Okayama, M. Machida, Adsorption of aqueous metal ions on cattle-manure-compost based activated carbons, J. Hazard. Mater. 170 (2009) 1119–1124.